IEEE Access
Multidisciplinary | Rapid Review | Open Access Journal

Received March 2, 2021, accepted April 1, 2021, date of publication April 12, 2021, date of current version April 27, 2021.

Digital Object Identifier 10.1109/ACCESS.2021.3072695

Enhanced State Estimation Based on Particle Filter and Sensor Data With Non-Gaussian and Multimodal Noise

THOMAS WILTS AND SABAH BADRI-HOEHERR

[1]Faculty of Computer Science and Electrical Engineering, Kiel University of Applied Sciences, 24149 Kiel, Germany

Corresponding author: Thomas Wilts (thomas.cimiega@fh-kiel.de)

ABSTRACT This paper presents a novel approach to state estimation based on particle filter dealing with measurement data effected by non-Gaussian, multimodal noise. The implementation focusses on autonomous underwater vehicles (AUVs) utilizing data of a magnetic compass and a mechanical scanning sonar for spatial navigation. Nowadays, particle filter approaches often require complicated feature extraction methods culminating in semantic interpretation of the data. This is not suitable for low-cost and low-weight AUVs, because these steps require high computational power. Therefore, efficient CPUs and higher power delivery are required. To test the novel approach, the algorithm is simulated in different scenarios with different parameters. Additionally, the filter is applied to real environment data. Finally, the performance is tested and evaluated by several methods. We demonstrate the computational efficiency and superiority of our method over other approaches through simulations.

INDEX TERMS Autonomous underwater vehicle, particle filter, sonar navigation, localization, feature extraction.

I. INTRODUCTION

A. MOTIVATION

In the last few decades the research of underwater environments supported by robots like remotely operated vehicles (ROVs) and AUVs has increased significantly due to the off-shore industry, monitoring of flora and fauna, geological mapping and many more applications. While ROVs still need an operator to control the vehicle, AUVs are capable of fulfilling a mission autonomously. On the other hand, AUVs require robust localization and navigation methods to deliver reliable data. Determined by the requirements, AUVs come in different sizes and capabilities. In this work, we are focussing on so called low-cost and low-weight AUVs, which implies sensors with less precise data and limited processing power. This makes the possibilities for navigation and localization difficult. Depending on the area of application, various localization methods are available and offer different benefits and disadvantages. Methods like long baseline (LBL) or short baseline (SBL) are very precise, but require a base station on the surface or previously deployed beacons. These methods are expensive, call for operators, and need extensive preparation. Alternative methods like simultaneous localization and mapping (SLAM) require a considerable amount of computational efforts to enable real time processing. One other solution, which is the basis of our work, is the so called particle filter. Particle filters enable a state space estimation of non-linear and multi-modal models. Through these advantages they have gained popularity in the robotic society. However, particle filters and similar estimation algorithms require adequate preprocessing of the data for satisfying interpretation. Depending on the sensor, such preprocessing consumes a high amount of energy and computational resources. Some examples are image-based preprocessing and complex non-linear filtering steps for denoising and recognizing expected objects in the sensor data. Using sonar data usually requires such filtering steps to reduce background noise, attenuation issues, volume reverberation, bottom- and surface hits, and mirroring effects. To deal with signals containing so called clutter, it requires individual and complex handling, because of ambiguous and unexpected varying number of possible results. In this work a promising way for localization with particle filters is presented. It is capable of handling vastly disturbed sensor data due to clutter

The associate editor coordinating the review of this manuscript and approving it for publication was Anton Kos.

phenomena and keeps the computational complexity low. This is demonstrated using a particle filter in combination with mechanical scanning sonar data of an AUV.

B. RELATED WORKS

Particle filters where first introduced 1993 by Gordon *et al.* [1] and became a popular solution for non-linear and multi-modal state estimation problems. One of the first simulations to localize AUVs were done by Karlsson *et al.* [2]. The first attempts to localize the position of an AUV were made by Maurelli *et al.* [3] with the RAUVER and a Tritech Seaking mechanical scanning sonar in a real underwater environment. After that different approaches succeeded such as those employing other kinds of sensors e.g. imaging sonar [4], [5], SLAM realizations [6]–[8] or those focussing on extensive landmark recognition and semantic interpretation of the data [9]. Each of these developments, although they were successful, increased the computational load thus requiring higher potential processor units. In contrast to that, there is also the trend for cheaper, smaller and durable AUVs for e.g. swarm operations [10]. Such AUVs, so called low-cost and low-power AUVs, are focussed in this work. Low-cost and low-power AUVs are often utilized in shallow water areas like harbours or lakes. This circumstance introduces clutter to the sonar sensor data. Previous works in the sonar, radar [11] and image-tracking [12] field of application presented reasonable results to deal with this issue. Liu *et al.* [11] also introduces four methods to deal clutter in similar conditions and will be used as benchmark for comparison. This paper is structured as follows: Section II describes the particle filter algorithm and the statistical approach. The simulated setup and the validation of the concept guided by the results are presented in section III. Here we acquired the Cramér-Rao bound (CRB) for a conventional particle filter approach and compared it with the enhanced approach and methods of [11] in terms of precision and convergence speed. In section IV results of a field trial are presented. Finally, section V summarizes the work and concludes with future works.

II. PARTICLE FILTER FOR LOCALIZATION

The main goal of this work is the position estimation of a low-cost and low-power AUV equipped with a mechanical scanning sonar using a particle filter. Besides the position, this realization also estimates a speed-error correction and a heading-error correction. This is necessary due to the lag of speed measurement via e.g. Doppler velocity log (DVL) and the usage of a magnetic compass or fibre-optic gyro, which tend to be unprecise, disturbed or gaining an offset over time.

The use of particle filters arises from the fact that they are suitable for models with non-linear systems and non-gaussian measurement noises. Compared to e.g. Kalman filters, they have a higher computational complexity, but Kalman filters suffer from the conditions in such scenarios [11]. To overcome this disadvantage in order to fit the lower computational power of low-power and low-weight AUVs, this work offers an enhancement of the classical particle filter approach. As presented in [13] the particle filter is a nonparametric Bayes filter. It is well suited to represent multimodal beliefs like the state space of robots such as AUVs. They are also capable of representing nonlinear processes like complex movement characteristics. Such circumstances prevail in the underwater domain [4].

The filter uses so called particles – possible state spaces $\mathbf{X}_t = \left[\mathbf{x}_t^{(0)}, \mathbf{x}_t^{(1)}, \ldots, \mathbf{x}_t^{(N-1)}\right]$ – whose density represents the probability of the current state $p(\mathbf{x}_t)$. The number of particles is defined by N. To acquire the current particle set $\mathbf{X}_t$, the previous particle state set $\mathbf{X}_{t-1}$ is updated by the influence of the current control input u_t and measurement z_t. By doing so, the density function of the particles approximates the estimated position distribution [14]:

$$p\left(\mathbf{x}_t\right) \approx \frac{1}{N} \sum_{n=0}^{N-1} \delta\left(\mathbf{x}_t - \mathbf{x}_t^{(n)}\right). \tag{1}$$

The basis of this particle filter is addressed in [14], which implementation is described in following steps: At first we initialize N particles to gather a random initial set of $\mathbf{X}_t$. The distribution of the initial states of the particles depend on the state definition and limits. An example for the initialization is shown in III. For each particle in the set $\mathbf{X}_t$ a weight is calculated by

$$\begin{aligned} w_t\left(\mathbf{x}_t^{(n)}, z_t\right) = w_t^{(n)} &= \mu w_{t-1}^{(n)} p\left(z_t \mid \mathbf{x}_t^{(n)}, m\right) \\ &= \mu w_{t-1}^{(n)} \sum_{n=0}^{N-1} e^{\left|z_t - f_z\left(\mathbf{x}_t^{(n)}, m\right)\right|}, \\ p\left(z_t \mid \overline{\mathbf{x}}_t, m\right) &\approx \mu \sum_{n=0}^{N-1} \underbrace{e^{\left|z_t - f_z\left(\overline{\mathbf{x}}_t^{(n)}\right)\right|}}_{w_t^{(n)}} \delta\left(\mathbf{x}_t - \overline{\mathbf{x}}_t^{(n)}\right), \end{aligned} \tag{2}$$

which is referred as *measurement update*. The measurement function $f_z(\cdot)$ is the expected measurement due to the particle state and m is the map. For better overview, m is omitted in the future equations but is still considered as dependency. The normalization factor μ scales the weights $w_t^{(n)}$ to

$$\mu \sum_{n=0}^{N-1} w_t^{(n)} = 1. \tag{3}$$

In the next step called *resampling* a new set of samples is generated. This is done by randomly picking particle indices n' out of the previous set, whereby particles with a high weight have a higher chance to be chosen:

$$P\left(n'\right) = \mu w_t^{(n')}\Big|_{n' \epsilon [0 \ldots N-1]}. \tag{4}$$

Thus leading to a new particle set

$$\mathbf{x}_t'^{(n)} = \mathbf{x}_t^{\left(n'^{(n)}\right)}. \tag{5}$$

Finally, a prediction of each particle is made by using the motion model function $f_x(\cdot)$ of the platform later introduced

in III:

$$\mathbf{x}_{t+1}^{(n)} = \overline{\mathbf{x}}_t^{(n)} = f_x(\mathbf{x}_t'^{(n)}, u_t) + \mathbf{y}_t \epsilon_t^{-1}, \tag{6}$$

with $\mathbf{y}_t$ as a random Gaussian distributed vector with zero mean and a tunable variance $\boldsymbol{\sigma}_{\mathbf{y}_t}$ and ϵ_t a measurement-error weight. Adding $\mathbf{y}_t$ generates varieties in the state space of the new particle set and ϵ_t forces convergence of the particles.

We define the error ϵ_t by the best ten percent of particles described by:

$$\epsilon_t = \frac{10}{N} \sum_{n=0}^{\frac{N}{10}-1} e^{\left|z_t - f_z\left(\mathbf{x}_t^{(n)}\right)\right|}, \tag{7}$$

where

$$e^{\left|z_t - f_z\left(\mathbf{x}_t^{(n)}\right)\right|} \leq e^{\left|z_t - f_z\left(\mathbf{x}_t^{(n+1)}\right)\right|}. \tag{8}$$

A. RANDOMIZED PICKING APPROACH STATISTICAL APPROACH

The novel idea of this work is the statistical choice of possible object detections. A major issue of the successful usage of particle filters is the precision of the measurement data z_t. In land or air robotics, often quite precise sensors provide reliable results and do not need any further preprocessing, whereas in the underwater domain the echoed signal of sonars need to be interpreted to distinguish features from clutter. Sonars are the most commonly used sensor types in the underwater domain. Here, various types like forward looking sonars, sidescan sonars or mechanical scanning sonars are employed. The latter of which constitutes the focus of the present work. They receive the echoes of a previously sent ping and provide the intensity of the received signal over range. After that the transducer rotates to measure the echoes from a different angle. Determining objects like walls out of the signal is a difficult matter during the preprocessing. The echo of such objects varies depending on its size, material, alignment, and range to the sonar. In general, a peak in intensity, caused by the reflected sound, following a falling edge, caused by the acoustic shadow, indicates an object. However, the reflected signal is disturbed by noise, multipath propagation and, the backscatter of the sea surface and bottom causing difficulties in the interpretation.

In Fig. 2 the non-linear relationship between the expected range to a reflecting object like a wall or underwater structure and the measured intensity of each sonar beam is shown. The sonar data are gathered from the Tritech Micron Mechanical Scanning Sonar [16] and a time-varying gain is applied to compensate spherical losses. It is clearly visible that reverberation disturbs the measurement and covers echoes from higher ranges. Achieving the range by extracting the highest intensity causes multimodal, non-Gaussian distributed measurement results. These disturbances need to be reduced in the preprocessing for particle filters, because false assumptions lead to wrong features for the position estimation. Several previous works towards sonar signal processing apply complex noise attenuation, pattern recognition, image processing for arbitrary shapes and objects, and a distinction of undesired signals like bottom and surface backscatter [5]–[7] or they disregard this issue [3], [17]. Nevertheless, these algorithms require computational power, which is limited on applications like AUVs. To tackle these issues, following assumptions are made: At first we assume, that the measured echo from desired objects are gaussian distributed, whereas clutter is assumed as nearly uniform distributed from zero to the maximum sonar range. This is only valid for a moving platform. For the second assumption, we define the state $\mathbf{x}_t^a$ and $\mathbf{x}_t^b$, where $\mathbf{x}_t^a$ is closer to the true state $\mathbf{x}_t$, thus

$$p(\mathbf{x}_t^a = \mathbf{x}_t) > p(\mathbf{x}_t^b = \mathbf{x}_t). \tag{9}$$

Next we define z_t^c as an echo from an undesired object, i.e. clutter and $z_t^{\neg c}$ as echo from a desired object. For the most time we also assume:

$$p\left(w_t\left(\mathbf{x}_t^a, z_t^{\neg c}\right) > w_t\left(\mathbf{x}_t^b, z_t^c\right)\right) > p\left(w_t\left(\mathbf{x}_t^a, z_t^{\neg c}\right) < w_t\left(\mathbf{x}_t^b, z_t^c\right)\right), \tag{10}$$

which means that the probability for having a high weight with a measurement $z_t^{\neg c}$ fitting the particle state $\mathbf{x}_t^a$ is higher than the probability of a clutter measurement z_t^c fits the particle state $\mathbf{x}_t^b$. If a measurement z_t^c coincidentially fits better to the particle state $\mathbf{x}_t^b$, we can further assume, that the probability of z_{t+1}^c fits particle state $\mathbf{x}_{t+1}^b$ again, is quite low. This is implied by the fact that the clutter is nearly independent of $\mathbf{x}_t$. These assumptions lead to the idea to randomly distribute the measured echoes $z_t^{\neg c}$ and z_t^c to the particles with states $\mathbf{x}_t^a$ or $\mathbf{x}_t^b$. After several iterations of weightening and resampling and due to Eq. 10 the particles converge to the true state $\mathbf{x}_t$. Additional to that the resampling step increases the probability $p(z_t^{\neg c}|\mathbf{x}_t^a)$, because if once the particle with state $\mathbf{x}_t^a$ gathered the measurement $z_t^{\neg c}$, its weight increases the chance to reproduce.

To realize this idea, the positions of all intensity peaks are extracted as features, assuming some of them could be the desired object reflections. Before extracting the peaks, a filter for denoising and peak enhancement is applied. This filter is realized as matched-filter which coefficients number and values match the typical length and shape of an acoustic echo from a wall. The K positions of local maxima in the enhanced signal $z_t^{(k)}$ with $k \epsilon [0 : K-1]$ are concatenated to a measurement vector $\mathbf{z}_t$. This feature extraction process is shown in Fig. 1. Depending on the map and the particles state, the measurement vector $\mathbf{z}_t$ contains peaks from noise, clutter, unmapped and thus unexpected object echoes or the expected, but noise disturbed echoes. At the *importance* step each particle assigns to one of the possible results by a random selection changing Eq. 2 to:

$$w_t^{(n)} = \mu \sum_{n=0}^{N-1} e^{\left|z_t^{\left(k^{(n)}\right)} - f_z\left(\mathbf{x}_t^{(n)}\right)\right|}, \tag{11}$$

with $P\left(k^{(n)}\right) = \frac{1}{K}$ and

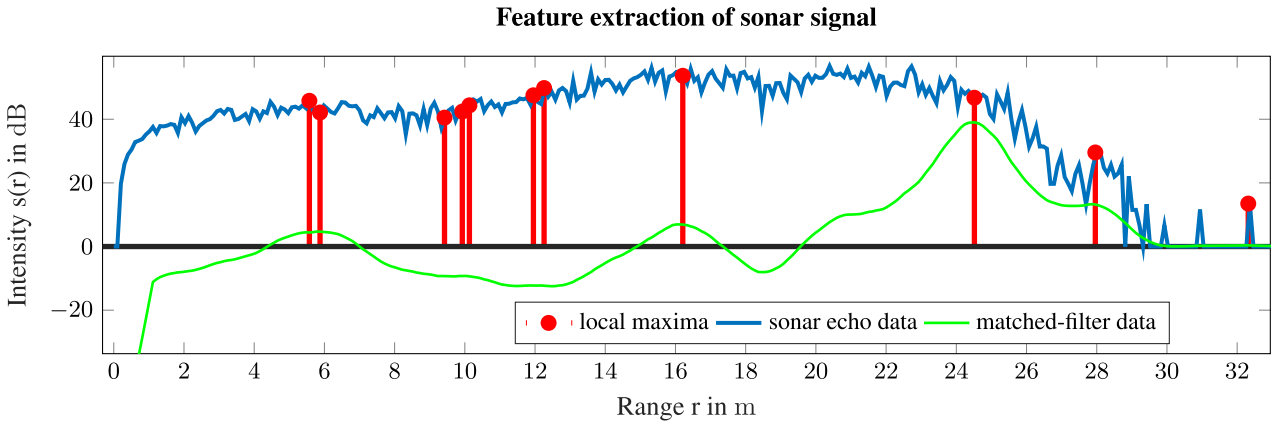

FIGURE 1. Preprocessing of sonar data. After enhancement (green) of the sonar signal (blue), the peaks z_t (red) are fed into the particle filter.

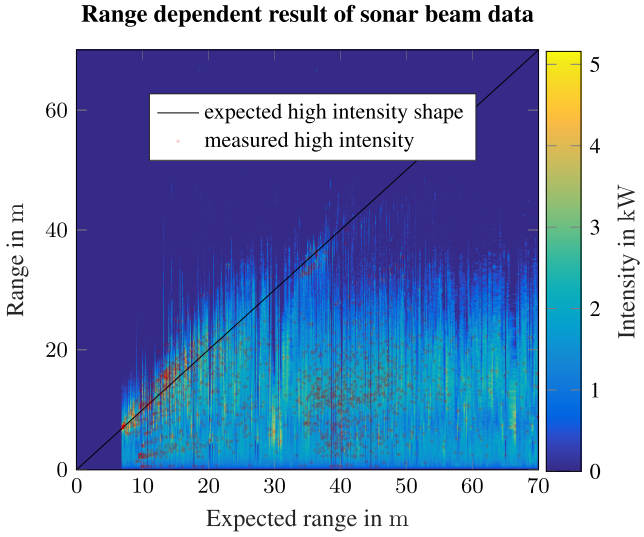

FIGURE 2. A set of sonar beam measurements sorted by the range to an object. The black line marks the expected shape of echo intensity depending on the range to an obstacle. The semi-opaque red dots mark the highest intensity of each beam, gathered from a converged particle filter introduced in this work. The data were recorded at the field trial described in section IV with the Tritech mechanical scanning sonar.

$$z_t^{(k)} = \arg\max_r \left(\frac{ds_t(r)}{dr} = 0, \frac{d^2 s_t(r)}{dr^2} < 0 \right), \qquad (12)$$

with $s_t(r)$ is the filtered sonar echo signal and r the range in meters. A further change is the deletion of $w_{t-1}^{(n)}$. Due to the random placement of the measurements, the *memorization* of previous weights has no positive effect. In some cases a particle does not expect any measurement from a mapped object, because the sensor does not point to any object in the map. In such cases the particles expected measurement $f_z\left(\mathbf{x}_t^{(n)}\right)$ is set to a random result between zero and the maximum sensor range. This special case will be demonstrated in section III by a scenario with sparse map features.

The aim of this modification introduced in Eq. 11 is to additionally let the particle filter figure out the optimal measurement option. By distributing the results over the particle set, only particles with matching measurement input and predicted state have a high chance to survive, whereas the chance of a wrong feature and a deviant predicted state match is very low. This allows to skip semantic preprocessing algorithm, that has to distinguish, which one of the possible returned echoes are the desired objects, clutter or noise. The presented method is capable of receiving an arbitrary amount of wrong results simultaneously, as long $K \ll N$. Obviously the amount of particles has to be increased with this approach, because only $\approx N/K$ particles receive the correct measurement assuming only one correct result is the measurement vector. According to that, the number of particles needs to be increased with the dimensionality of the particle state space [13]. Otherwise a slower convergence – if at all – to a satisfying estimation has to be taken into account. This increment has to be larger the higher the average number of peaks in the feature vector. A result of an analysis according to the required increase of particles is shown in III.

On the other hand, this realization brings several benefits: As previously shown, the preprocessing takes less implementation effort. Also only simple preprocessing steps are sufficient and do not tend to create incorrect features and sparse parameters. Besides the simplicity of implementation, this method reduces the processor load compared to algorithms using image processing algorithms and landmark detection, where single pings of a sector are stiched together to an image and validated in several stages with non-linear filter steps [6], [7]. The latter is especially important in low-cost AUVs, which are limited in energy consumption and thus computational load.

B. ALTERNATING STATE SPACE TO REDUCE THE NUMBER OF PARTICLES

As mentioned before, the particle filter estimates the spatial position, the percentage speed error, and the heading error $\hat{\mathbf{x}}_t = \left[\hat{x}_{\mathrm{x},t}, \hat{x}_{\mathrm{y},t}, \hat{x}_{\Delta\mathrm{v},t}, \hat{x}_{\Delta\theta,t}\right]^T$. The reason for estimating the percentage speed error results by the assumption that the percentage error of the speed varies less than the

speed itself. Furthermore, it is assumed that the particle filter itself catches wrong estimates of the percentage speed error by the position variance, introduced in Eq. 6 with $\mathbf{y}_t = \left[y_{\mathrm{x},t}, y_{\mathrm{y},t}, y_{\Delta\mathrm{v},t}, y_{\Delta\theta,t}\right]^T$.

Initially the variance $\mathrm{var}\left(y_{\mathrm{x},t}\right)$ and $\mathrm{var}\left(y_{\mathrm{y},t}\right)$ should be high to reduce premature clustering of particles. This enables the initialization of $\mathrm{var}\left(y_{\Delta\mathrm{v},t}\right) \ll \mathrm{var}\left(y_{\mathrm{x},t}\right)$ and $\mathrm{var}\left(y_{\Delta\mathrm{v},t}\right) \ll \mathrm{var}\left(y_{\mathrm{y},t}\right)$. Allowing only small correction steps at non-converged state synthetically reduces the particle filters state space. As a result, the number of particles can be reduced. After convergence of location states of the particle set, the variance of $y_{\Delta\mathrm{v},t}$ can be increased. For the heading error it is assumed that the magnetic sensor has the most accurate measurement at the beginning of the simulation and starts to diverge and gets disturbed after mission start. Consequently the variance $\mathrm{var}\left(y_{\Delta\mathrm{v},t}\right)$ will be increased over time and thus by convergence. To realize this behaviour for $y_{\Delta\theta,t}$ and $y_{\Delta\mathrm{v},t}$, the variances are slightly modified by a sigmoid function, explained by:

$$\mathrm{var}\left(y_{\Delta\theta,t}\right) = \sigma_{y_{\Delta\theta,t}}\,\mathrm{sig}\left(-\log_{10}\left(\frac{\epsilon_t}{c_{\min}}\right)\right), \tag{13}$$

here $c_{\min}$ is a specific convergence border. For this particular examples the convergence border is defined as $c_{\min} = 0.5\,\mathrm{m}$. This value may change for different map scales. This procedure leads to estimating the speed and heading error after convergence of the position.

III. EVALUATION AND ANALYSIS

A. AUV SETUP AND SCENARIO

At first, the new approach is tested for an AUV using a mechanical scanning sonar. To find suitable parameters and evaluate the new approaches an AUV simulation framework was built in MATLAB®. The simulation provides synthetic magnetic sensor data with adjustable noise amplitude and offset increase:

$$h_t = \theta_t + n_{\mathrm{yaw},t} + b_{\mathrm{yaw},t} \tag{14}$$

with θ_t as the true yaw, $n_{\mathrm{yaw},t}$ as Gaussian noise and $b_{\mathrm{yaw},t}$ as increasing offset at each time step. The speed control is provided by u_t and results in a diverging speed of:

$$v_t = u_t\left(1 + d_{\mathrm{speed},t}\right) + n_{\mathrm{speed},t}, \tag{15}$$

with $0 < d_{\mathrm{speed},t} < 1$ as fixed speed error and $n_{\mathrm{speed},t}$ as Gaussian noise with zero mean. This specific error emulates the lag of speed control. Thus only the thrust of the simulated AUV can be set assuming a linear relation to the resulting speed. Due to unknown fluid resistance, the achievable speed is lower than expected in calm water most of the time. Instead of simulating the channel response of the sonar, the resulting features from the feature extraction are provided:

$$\mathbf{z}_t = [z_t^{(0)}, z_t^{(1)}, \ldots, z_t^{(k)}, \ldots, z_t^{(K-1)}], \tag{16}$$

where most $z_t^{(k)}$ are a random number from zero to the maximum sonar range. One element of the vector contains the true range measurement added with a Gaussian noise with a variance of 0.5 m. Like in real scenarios, the number of found peaks varies resulting in K being a random integer between the minimum and maximum expected amount of peaks. Additionally, some fixed peaks are added to simulate first bottom and surface hits and other strong correlated interferer.

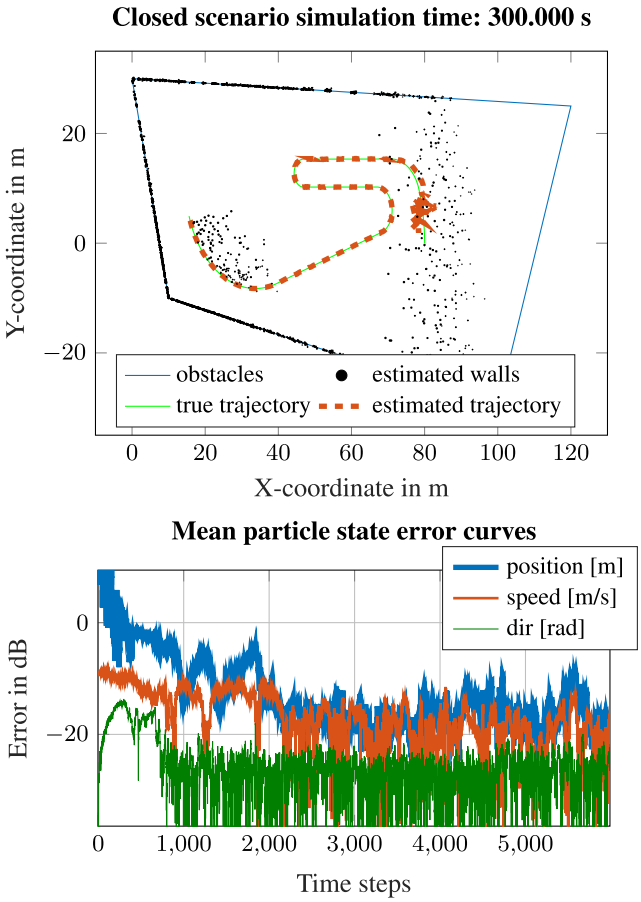

FIGURE 3. Simulation result of the closed scenario with upper limit $K = 50$ and $N = 2000$. Top: The wall estimations (black dots) are buffered for the last 3000 pings. The AUV started at the right side. Bottom: The error curves for each state per time step (x- and y-position error are calculated by the euclidian distance).

The state of the simulated AUV is the spatial position in two dimensions. The motion model of the AUV is described as:

$$\mathbf{x}_t = \mathbf{A}_m\mathbf{x}_{t-1} + \mathbf{B}_m(\theta_t)\,v_t + \boldsymbol{\sigma}_{m,t}, \tag{17}$$

with $\mathbf{A}_m$ as state transition matrix, $\mathbf{B}_m(\theta_t)$ as heading dependent control input matrix and $\boldsymbol{\sigma}_{m,t}$ as process noise vector. The state of each particle is simulated by four variables: the two dimensional position $x_{x,t}^{(n)}$ and $x_{y,t}^{(n)}$, heading correction $x_{\mathrm{yaw},t}^{(n)}$ and percentage speed correction $x_{\mathrm{speed},t}^{(n)}$. The prediction of each particle is implemented as:

$$\begin{aligned}\mathbf{x}_t^{(n)} &= f_x(\mathbf{x}'^{(n)}_{t-1}, u_{t-1}) \\ &= \mathbf{A}\mathbf{x}_{t-1}^{(n)} + \mathbf{B}\left(h_t + x_{\mathrm{yaw},t-1}^{(n)}\right)\left(1 + x_{\mathrm{speed},t-1}^{(n)}\right)u_t.\end{aligned} \tag{18}$$

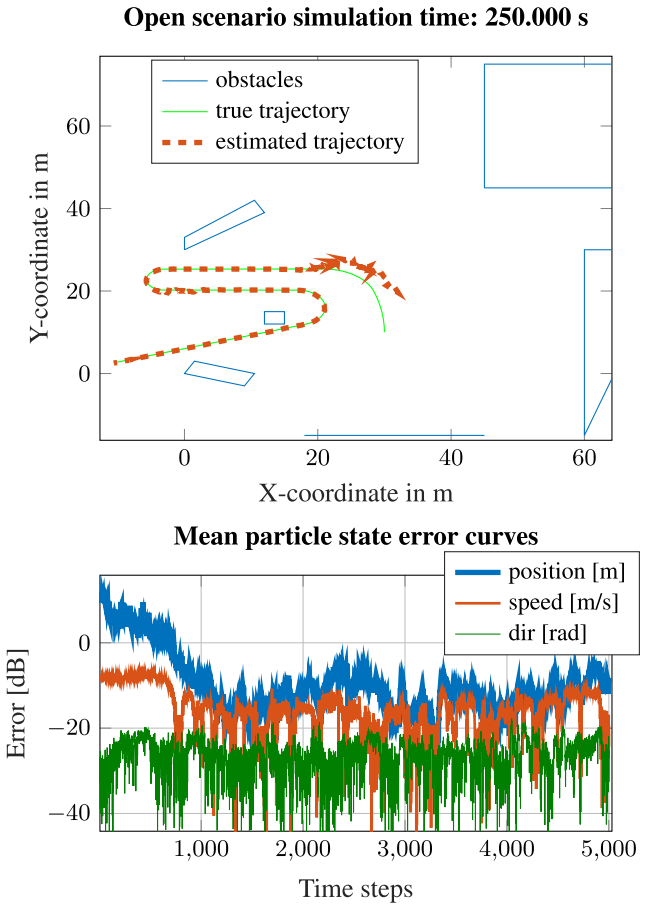

FIGURE 4. Simulation result of the open scenario with upper limit $K = 50$ and $N = 2000$. The wall estimations are buffered for the last 3000 pings. The AUV started at the right side.

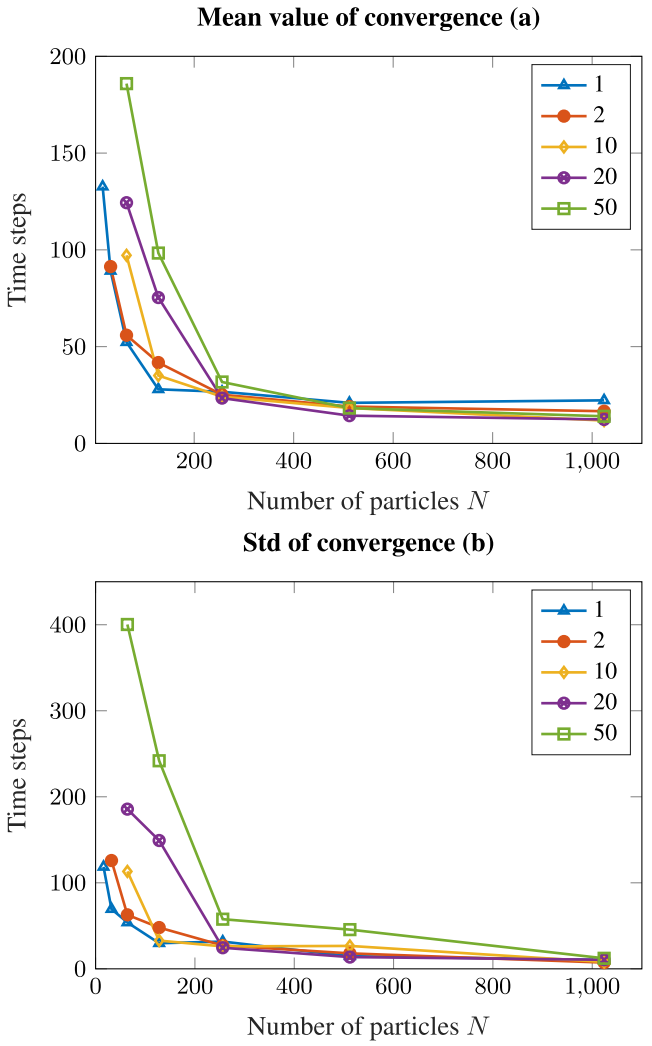

FIGURE 5. Convergence of particle filter with varying number of particles and sizes of the result vector $z_t^{(k)}$: (a) describes the mean value over 100 simulations and (b) the standard deviation.

Note that $\mathbf{B}(\cdot)$ is a function depending on the current particles yaw. After setting all parameters, a control command list defining speed and change of yaw for each time step can be configured. The estimated position is determined by the average position of ten percent of the particles with the highest weights.

B. NUMERICAL RESULTS

Two simulation scenarios were picked to test the behaviour of the particle filter. The first scenario, see Fig. 3, is a quadrilateral basin with no parallel edges. This guarantees a nearly continuous measurement relating to the map and the asymmetrical shape reduces spatial ambiguities. The AUV moves in different motion patterns with varying turn rates $\dot{\theta} \in \left[1\,^\circ\,\mathrm{s}^{-1}, \ldots, 9\,^\circ\,\mathrm{s}^{-1}\right]$ and speeds $u_t \in \left[0.1\,\mathrm{m\,s}^{-1}, \ldots, 0.6\,\mathrm{m\,s}^{-1}\right]$. The sonar has a maximum range of $R = 70\,\mathrm{m}$ and a ping rate of $20\,\mathrm{s}^{-1}$. The initial particles were spread homogeneously inside the quadriteral facing in an arbitrary direction. The second scenario, see Fig. 4, uses the same motion pattern, but the environment consists of medium sized and randomly placed obstacles. This scenario emulates an area with less spatial information resulting in $\mathbf{z}_t$ only containing undesired measurements. In this scenario the initial particles were distributed inside the edges of the axes and again facing in any arbitrary direction.

The new approach shows a satisfying convergence behaviour for both scenarios with 800 steps for the closed scenario and 1500 steps for the open scenario having at most $K = 50$ elements in the measurement vector. Also the speed and heading error estimation operated as expected. It is clearly visible, that the open scenario converges slower due to the sparse spatial features from the map. To measure the required amount of particles a measurement series with varying K at increasing number of particles is provided in Fig. 5. This shows especially the difference of errorless measurements ($K = 1$) and an expected amount of erroneous peaks in the sonar signal ($K = 50$).

C. ANALYTICAL STUDY WITH Cramér-RAO BOUND

To prove the enhanced performance of the presented approach, a comparison of the performances with different distributions of adequate measurements and false

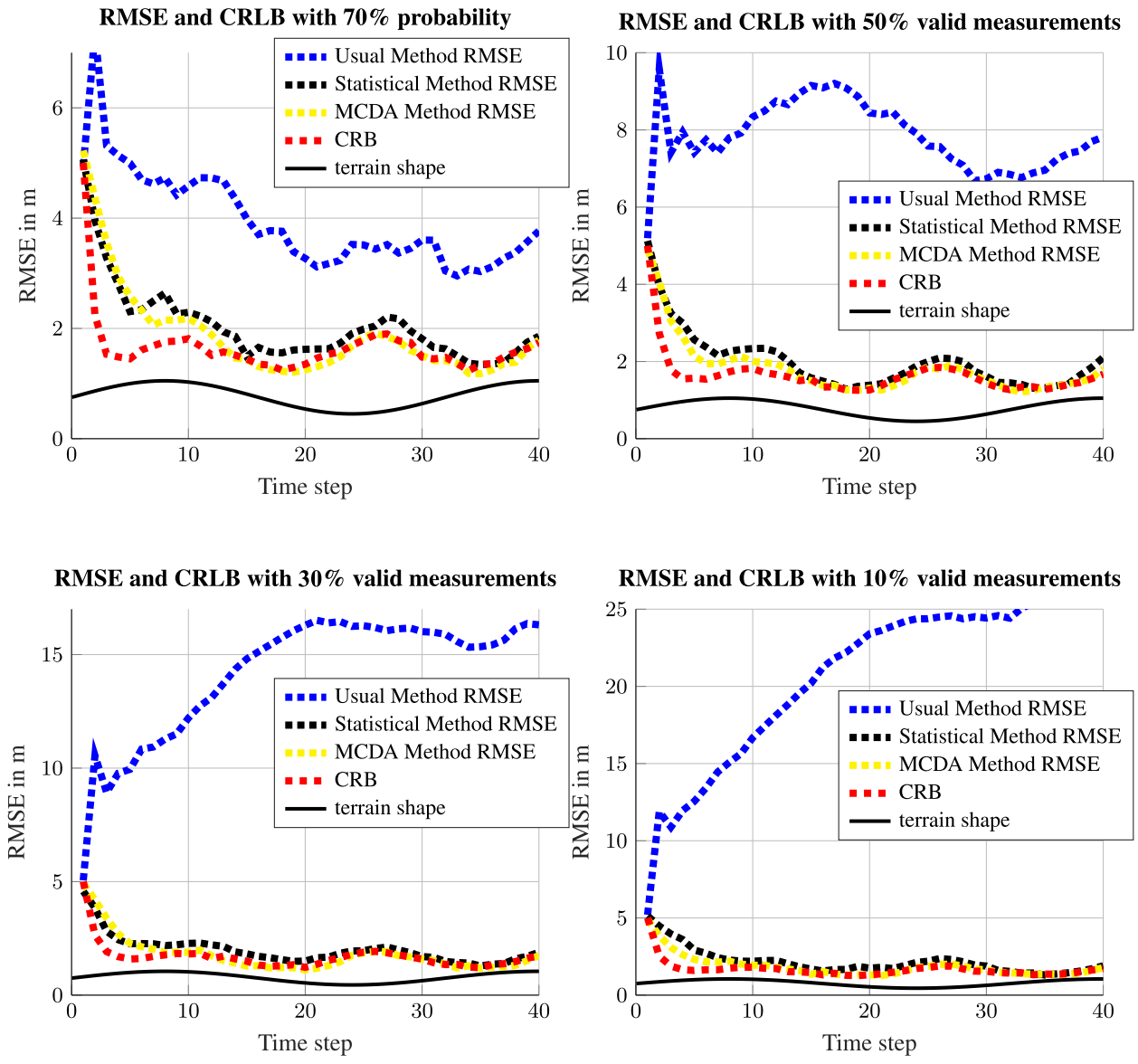

FIGURE 6. Numerical result of the RMSE and CRB for different distributions of desired and false measurements. The terrain curve describes the height map.

measurements is performed with another simulation in MATLAB®. Three different approaches are compared: The first one chooses a random result $z_t^{(k)}$ of vector $\mathbf{z}_t$ for all particles as measurement input and the second processes the result vector as described in Eq. 11. The third, called Monte-Carlo data association (MCDA), is taken from [11], where several particle filter methods where introduced and compared. The MCDA method calculates the particle weight by summing the likelihood of possible measurement combinations. The measurement vector contains one true, Gaussian noise disturbed measurement and at most $K-1$ random measurements. These random measurements are limited to the maximum sensor range. The RMSEs of all particle state estimations are compared. Furthermore the CRB is estimated due to the work of Kim and Bang in [18]. Their work utilizes simultaneous perturbation as described in [19] to estimate the Fisher information matrix known as the inverse of the CRB. To reduce computational complexity, a one dimensional system taken from [18] is applied. In this example a hovering object is moving along the horizontal direction and takes height measurements of a known height map. This simple example allows to gather a suitable amount of simulation results and thus a good average. For this particular measurement series each measurement was repeated 500 times using $N = 1000$ particles and an upper limit of $K = 20$. In Fig. 6 the results show that the novel approach can handle the non-Gaussian, multimodal noise of the sensor data. The particles converge close to the estimated CRB. Noticeable are the constant results for the CRB and that the particle filter always stays close to it for all tested distributions

TABLE 1. Required simulation calculation time under equal parameters.

measurement	first	second	third	fourth	mean
presented method	44.73 s	44.84 s	65.10 s	47.45 s	50.53 s
MCDA	91.95 s	91.87 s	140.88 s	93.96 s	104.66 s

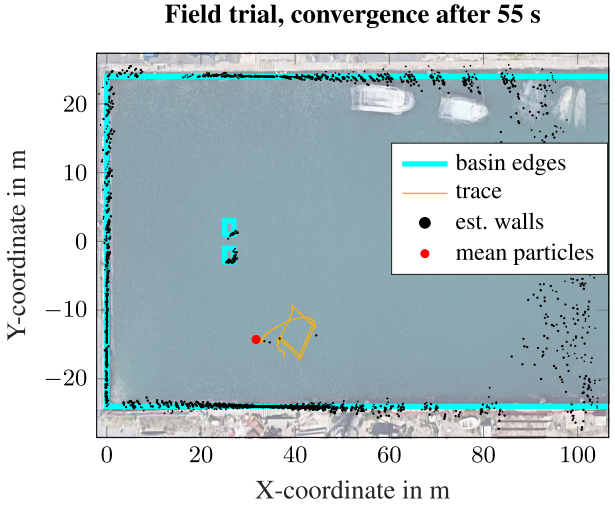

FIGURE 7. Testing the particle filter in a harbour area in La Spezia. The AUV was supposed to drive in a rectangular trajectory. The filter converged after 54 s. After the last turn the vehicle was pulled out of the water. The map is taken from [22].

of desired and false measurements. Only the convergence time extends with increasing amount of false measurements. In comparison to that, the default particle filter has a much higher error for a 50 percent chance measuring the desired range or even diverges for lower percentages. The MCDA method was always the most precise one, but the calculation time was always more than double the calculation time of the presented method as shown in Tab. 1. Compared to all methods introduced in [11], the presented method is the most unprecise, but fastest one.

IV. FIELD TRIALS

To test the new approach in a real scenario, data from runs at the European Robotics League (ERL) 2019 in La Spezia were used and fed into the particle filter algorithm. Unfortunately we were not able to precisely track the true position due to missing localization sensors. Instead, the true position is estimated by comparison of the observations during the run and the map.

A. TEST SCENARIO

The test took place at the Centre for Maritime Research and Experimentation in La Spezia in a 48 m times 120 m sized basin. A large structure was centred inside the basin. Due to its symmetrical shape, the initial position of the particles where restricted to the lower half of the basin to avoid ambiguities. The Rucksack AUV, manufactured by the AUV Team TomKyle [20], was equipped with a Tritech mechanical scanning sonar [16] set to 360 degree sector scan, highest rotation rate of $10.45\,^\circ\,\mathrm{s}^{-1}$ and a ping rate of $8.45\,\mathrm{s}^{-1}$. The Rucksack AUV is equipped with an UP Squared board using an Intel Pentium N4200 processor [21]. The AUV path was programmed to perform rectangular shaped trajectories.

B. OUTCOME

The trial shows a convergence after 54 sec and a trajectory performed as expected. At the beginning, the particle filter did not manage to find an unambiguous result, but one of the denser particle heaps indicated the outcome position. This could be resolved by back propagating from the converged trace. However, this step would imply a posteriori knowledge, which is not focus of this work, due to real time capability of the algorithm. The area close to the stairs at the lower side of the map and distance from the lower wall 5 m and 42 m from the left wall matches the observations.

V. CONCLUSION

This paper illustrated a simple modification of particle filters, which enables to perform under the condition of cluttered sensor data e.g. from sonars. Simulations show the ability of convergence even if the amount of wrong measurements is relatively high. Also the implementation requires lower computing power compared to complex image processing algorithms. Thus, it reserves more capabilities for other computing tasks and has a lower energy consumption. This fact is important especially in battery powered robots like AUVs. The provided method shows a negligible increase of the amount of particles for spatially open and closed scenarios supported by using a method to initially reduce the state space. After complete convergence of the filter, the state accuracy was sufficient enough for applications like AUVs.

A. FUTURE WORK

Following improvements may be realised in the future. First, several methods like an adaptive particle number [23], random creation [5] or other basic improvements can be implemented. Second, the algorithm could be expanded with SLAM methods to navigate without a known map as described in [6], [17]. At last, the sonar could be exchanged by an imaging sonar. By doing so, each beam can be preprocessed as before and fed simultaneously into the particle filter. By receiving spatial information from several directions, the particle filter should converge faster and more robustly.

ACKNOWLEDGMENT

We acknowledge financial support by Land Schleswig-Holstein within the funding programme Open Access Publikationsfonds.

REFERENCES

[1] N. J. Gordon, D. J. Salmond, and A. Smith, Eds., "Novel approach to nonlinear/non-Gaussian Bayesian state estimation," *IEE Proc.-F*, vol. 140, no. 2, 1993.

[2] R. Karlsson, F. Gustafsson, and T. Karlsson, Eds., "Particle filtering and cramer-rao lower bound for underwater navigation," in *Proc. IEEE Int. Conf. Acoust., Speech, Signal Process. (ICASSP)*, 2003.

[3] F. Maurelli, S. Krupinskiy, Y. Petillot, and J. Salviz, "A particle filter approach for AUV localization," in *Proc. OCEANS*, Quebec City, QC, Canada, Sep. 2008, pp. 1–7.
[4] F. Maurelli, A. Mallios, D. Ribas, P. Ridao, and Y. Petillot, Eds., "Particle filter based AUV localization using imaging sonar," in *Proc. 8th IFAC Int. Conf. Manoeuvring Control Marine Craft*, Guarujá, Brazil, Sep. 2009.
[5] F. Maurelli and S. Krupinski, "A semantic-aided particle filter approach for AUV localization," 2019, *arXiv:1905.07470*. [Online]. Available: http://arxiv.org/abs/1905.07470
[6] D. Romagós, P. Ridao, and J. Neira, *Underwater SLAM for Structured Environments Using an Imaging Sonar*, vol. 65. Berlin, Germany: Springer-Verlag, Jan. 2010.
[7] D. Forouher, J. Hartmann, M. Litza, and E. Maehle, "Sonar-based FastSLAM underwater environ. Using walls as features," in *Proc. 15th Int. Conf. Adv. Robot. (ICAR)*, Tallinn, Estonia, Jun. 2011, pp. 588–593. [Online]. Available: http://ieeexplore.ieee.org/servlet/opac?punumber=6081304
[8] M. Choi, R. Sakthivel, and W. K. Chung, "Neural network-aided extended Kalman filter for SLAM problem," in *Proc. IEEE Int. Conf. Robot. Automat.*, Roma, Italy, Apr. 2007.
[9] S. C. Brian, "The resampling weights in sampling-importance resampling algorithm," M.S. thesis, Dept. Statist., Chin. Univ. Hong Kong, Hong Kong, Jul. 2016.
[10] A. Amory, B. Meyer, C. Osterloh, T. Tosik, and E. Maehle, "Towards fault-tolerant and energy-efficient swarms of underwater robots," in *Proc. IEEE Int. Symp. Parallel Distrib. Process., Workshops Phd Forum*, May 2013, pp. 1550–1553.
[11] B. Liu, C. Ji, Y. Zhang, C. Hao, and K.-K. Wong, "Multi-target tracking in clutter with sequential monte carlo methods," *IET Radar Sonar Navigation*, vol. 4, pp. 662–672, 11 2010.
[12] M. Isard and A. Blake, "Condensation—Conditional density propagation for visual tracking," *Int. J. Comput. Vis.*, vol. 29, pp. 5–28, Aug. 1998.
[13] S. Thrun, W. Burgard, and D. Fox, "Probabilistic Robotics," in *Intelligent Robotics and Autonomous Agents Series*. Cambridge, U.K.: MIT Press, 2006.
[14] F. Gustafsson, F. Gunnarsson, N. Bergman, U. Forssell, J. Jansson, R. Karlsson, and P.-J. Nordlund, "Particle filters for positioning, navigation, and tracking," *IEEE Trans. Signal Process.*, vol. 50, no. 2, pp. 425–437, Aug. 2002.
[15] C. Stachniss. *Basic Techniques: Chapter 2*. Accessed: Mar. 12, 2021. [Online]. Available: http://ais.informatik.uni-freiburg.de/teaching/ss13/robotics/
[16] Tritech Micron Mechanical Scanning Sonar. *Tritech*. Accessed: Mar. 12, 2021. [Online]. Available: https://www.tritech.co.uk/product/small-rov-mechanical-sector-scanning-%sonar-tritech-micron
[17] J. Tardós, J. Neira, P. M. Newman, and J. J. Leonard, Eds., "Robust mapping localization indoor environments using sonar data," *Int. J. Robot. Res.*, vol. 21, no. 4, pp. 311–330, Apr. 2002.
[18] Y. Kim and H. Bang, Eds., "Monte-Carlo calculation of cramer-rao bound for non-Gaussian recursive filtering," in *Proc. Asia–Pacific Int. Symp. Aerosp. Technol.*, Seoul, South Korea, 2017.
[19] J. C. Spall, "Adaptive stochastic approximation by the simultaneous perturbation method," *IEEE Trans. Autom. Control*, vol. 45, no. 10, pp. 1839–1853, Oct. 2000.
[20] A. T. TomKyle. *Rucksack AUV*. Accessed: Mar. 12, 2021. [Online]. Available: https://auv-team-tomkyle.de/?page_id=174
[21] UP. *Up Squared*. Accessed: Mar. 12, 2021. [Online]. Available: https://up-board.org/upsquared/specifications/
[22] Google maps. (2019). *La Spezia*. Nashville, TN to Santa Rosa Beach, FL, USA. [Online]. Available: maps.google.com
[23] P. Abbeel. (2019). *Particle Filters++*. Presentation, UC EECS, Berkeley. [Online]. Available: https://people.eecs.berkeley.edu/~pabbeel/cs287-fa11/slides/particle-fi%lters++_v2.pdf

THOMAS WILTS received the MSc. degree in electrical engineering and information technology from CAU, Kiel, in 2017. He is currently pursuing the Ph.D. degree in sonar navigation for autonomous underwater vehicles with the Kiel University of Applied Sciences (UAS). Since 2019, he has been a Research Assistant with UAS. His research interests include sonar data process-ing, artificial intelligence for autonomous under-water vehicles, and sonar mapping.

SABAH BADRI-HOEHER has been a Professor with the Faculty of Computer Sciences and Electrical Engineering, Kiel University of Applied Sciences, since 2009. Before, she has been with the Fraunhofer Institute for Integrated Circuits, Erlangen, Germany, and the Christian-Albrechts-University of Kiel for several years. She is currently a Researcher and a Technical Supervisor with the AUV Project. Her research interests include signal processing and communication techniques with focus on underwater applications.